

(p, γ) Resonance-Curve Shapes and Measurements of Resonance Energies with H_2^+ Beams

R. O. BONDELID AND J. W. BUTLER*

Nucleonics Division, U. S. Naval Research Laboratory, Washington, D. C.

(Received 27 May 1963)

The observation of an apparent nonlinearity in the NRL 2-m radius electrostatic analyzer has led to an exhaustive investigation of (p, γ) resonance-curve shapes induced by the hydrogen molecular-ion beam. The midpoint of the rise in the thick-target yield curve obtained with the H_2^+ beam, $Al^{27}(p, \gamma)$ reaction at 992 keV, was observed to be 0.05% lower than that predicted from the corresponding observation with the H_1^+ beam. When extremely thin targets were used, the energy coordinates of the peaks of the H_1^+ and H_2^+ yield curves agreed within 0.01%. Further studies with the H_2^+ beam revealed additional deviations from expected behavior. The thick-target yield curve was seen to be asymmetric about the midpoint; there was a hump or peak near the top of the thick-target yield curve. The peaks of moderately thin-target yield curves were not shifted from resonance energy by as much as half the target thickness in energy loss units; the full widths at half-height of these moderately thin-target yield curves were greater than predicted from the full width at half-height of an extremely thin-target H_2^+ beam yield curve and the target thicknesses in energy loss units obtained with the H_1^+ beam on the same targets. The energy shifts and broadening effects of inert coatings of copper over the aluminum targets were significantly different for H_1^+ and H_2^+ beams with both beams referred to the same energy scale; and even greater broadening, but not midpoint displacement, was observed with H_1^+ and H_1^0 components stripped from the H_2^+ beam in a gas cell. These deviations from expected behavior are all explained on the basis of the mechanism of dissociation of the H_2^+ molecule, and the results are applied to calibration of beam deflection analyzers.

I. INTRODUCTION

THE use of (p, γ) resonance reactions for calibration purposes is quite common because of the experimental simplicity of the measurements and also because of the relative lack of ambiguity in the interpretation of the data if the resonance is sharp. It has become commonly accepted practice to choose the midpoint of the rise in the thick-target yield curve as the resonance energy. This procedure, developed for use with proton (H_1^+) beams, has been extended by many nuclear-reaction physicists to include hydrogen molecular-ion (H_2^+) beams with only one significant conceptual difference. The internal motion of the two protons with respect to the center-of-mass of the H_2^+ molecule has been assumed to give a "Doppler" broadening in the effective energy inhomogeneity of the bombarding beam.

One practical application of the hydrogen molecular-ion beam is its use for energy *calibration* purposes. For electrostatic analyzers the same resonance whose energy is precisely known can be observed by both the H_1^+ and H_2^+ beams, and the calibration point for the H_2^+ beam is a factor of 2 higher (on the same energy scale) than that for the H_1^+ beam (except for the energy carried by the electron and the correction due to the stray magnetic field). For magnetic analyzers, the H_2^+ beam gives a calibration point a factor of 4 higher (on the energy scale) than the H_1^+ beam. The "Doppler" broadening of the rise in the thick-target step does not appear to affect the accuracy to a large extent because the midpoint of the rise can still be determined quite precisely. Such measurements also have been used to

test the energy *linearity* of electrostatic analyzers and the momentum linearity of magnetic analyzers.

Historically, the present series of investigations was initiated by the observation of an apparent nonlinearity in the NRL 2-m electrostatic beam-energy analyzer. The apparent energy of the 992-keV resonance in the $Al^{27}(p, \gamma)$ reaction, determined from the midpoint of the rise in the thick-target yield curve with the hydrogen molecular-ion beam, was lower than anticipated from the measurements with the proton beam, the amount of the "discrepancy" being about 0.05%.¹ All of the usual corrections, the relativistic effect, internal and external magnetic fields, and energy carried by the electron, were made to the raw experimental data before the situation was labeled a discrepancy. Since this discrepancy was greater than the expected relative uncertainty, considerable effort was expended in an attempt to find its source.

As sometimes happens when an intensive effort is made to discover the nature of one "discrepancy," or "anomaly," other "anomalies" are found. The next anomaly noted as a result of very detailed work was that the thick-target H_2^+ beam-yield curve is not symmetric about the midpoint of the rise. The bombarding energy interval required for the curve to rise to the midpoint is much greater than the interval required for the curve to rise from the midpoint to the apparent beginning of the thick-target plateau. More precise shape determinations revealed still another anomaly, the presence of a hump at the top of the rise.

When thin targets were used to make an independent check of the beam-energy analyzer calibration parameters in an effort to determine with certainty whether

* Present address: Department of Physics and Astronomy, Michigan State University, East Lansing, Michigan.

¹ R. O. Bondelid, J. W. Butler, and C. A. Kennedy, *Bull. Am. Phys. Soc.* 2, 381 (1957).

the original energy discrepancy with H_2^+ beams on thick targets was due to some unconsidered factor affecting analyzer linearity, yet another anomaly was observed: The experimental peaks in the yield curves of the thin targets did not shift with target thickness according to another commonly accepted practice which is to subtract half of the target thickness in energy-loss units from the energy coordinate of the peak and to assign the result to be the resonance energy.

Anomalies similar to those listed above were subsequently observed with H_1^+ beams and are reported elsewhere.² The anomalies with H_1^+ beams have all been explained by the application of the theory of fluctuations in energy loss and by the assumption of the existence of contaminating films covering the face of the target. The primary explanation for the H_2^+ beam anomalies is quite different from that used for the H_1^+ beam anomalies because of the nature of the dissociation mechanism of the hydrogen molecular ion.

II. EXPERIMENTAL APPARATUS

The positive-ion-beam acceleration was performed by the NRL 5-MV Van de Graaff accelerator; the beam analysis was accomplished (in most of the measurements) by a high-resolution 2-m electrostatic beam-energy analyzer; and the proton-capture gamma rays were detected (in most of the measurements) by a 3-in.-diam \times 3-in.-NaI(Tl) scintillation crystal with associated electronic equipment. The entire system is described in detail in other communications.^{3,4}

During the course of the experiments, various specialized pieces of apparatus were used, some of which are a gas cell for stripping the H_2^+ beam into its atomic components (H_1^+ and H_1^0), an associated permanent magnet mass- and charge-component separator, and a phototube circuit for measuring the relative amounts of the H_1^0 beam by means of its fluorescence properties with a quartz beam stopper.

The target-making procedure, described in detail elsewhere,⁵ may be briefly outlined as follows: The basic backing material, microscope slide glass, was first coated with an evaporated layer of copper, then the aluminum target material was deposited onto the copper. Usually seven targets were made simultaneously, the geometric arrangement in the evaporator system causing each target to differ in thickness from its neighbors by about a factor of 2. The most important series of targets has a thickness range from 17.8 to 0.31 keV for 1-MeV protons. These targets are labeled E-1 through E-7, in order of decreasing thickness.

The target holder is similar to one previously de-

scribed,⁶ including a tube kept at liquid-nitrogen temperature enclosing the target. This tube is of critical importance to the present series of experiments because of the possible displacement of the energy of a resonance by the presence of a film of inert or contaminating material on the target face.

III. EXPERIMENTAL RESULTS

For most of the measurements with the H_2^+ beam and the electrostatic analyzer, the beam-energy spread was 0.02%.

A. Displacement

As mentioned previously, the series of experiments reported herein was originally initiated by the observation that the midpoint of the rise of the hydrogen-molecular-ion-beam thick-target yield curve occurred at an energy about 0.05% lower than anticipated from the electrostatic analyzer readings for the same resonance observed with the proton beam. An apparent discrepancy of this magnitude was considered to be important because we had measured the absolute calibration parameters of the electrostatic analyzer with great precision. These parameters are the terms appearing in the absolute calibration equation,⁴ which is

$$eV_0 = V_p (e/k) (r_a/2d) (1+\gamma) (1+\epsilon_{\text{int}}) \times (1+\epsilon_{\text{ext}}) (1-nm_e/M_t), \quad (1)$$

where eV_0 is the energy of each proton incident on the target, k is the number of protons in the analyzed particle, V_p is the total voltage on the deflecting plates of the analyzer, d is the plate separation, and r_a is the arithmetic mean radius of curvature of the plates. The quantity $(1+\gamma)$ is the relativistic correction factor. The quantities $(1+\epsilon_{\text{int}})$ and $(1+\epsilon_{\text{ext}})$ are correction factors arising from the internal (within the region of the gap) magnetic field and the external (between the input slit and collimating slit) magnetic field, respectively. The terms ϵ_{int} and ϵ_{ext} are inversely proportional to $(M_t V_0)^{1/2}$, where M_t is the rest mass of the analyzed particle. The quantity n is the number of electrons in the analyzed particle and the correction term for the energy carried by these electrons is $(1-nm_e/M_t)$. All of the above correction factors are the same order of magnitude as the apparent discrepancy, several hundredths of a percent; hence, each correction factor must be determined carefully.

A re-examination of the parameters in Eq. (1) did not reveal a source of nonlinearity in the electrostatic analyzer; however, there are many other experimental factors or conditions which could conceivably influence the apparent value of the resonance energy. Therefore, many possible contributing effects were considered and shown either by calculation or by experiment not to be responsible for the discrepancy. A complete list of these

² R. O. Bondelid and J. W. Butler, Phys. Rev. **130**, 1078 (1963).

³ K. L. Dunning, R. O. Bondelid, L. W. Fagg, C. A. Kennedy, and E. A. Wolicki, NRL Progr. Rept. 1955, p. 8. (unpublished).

⁴ R. O. Bondelid and C. A. Kennedy, Phys. Rev. **115**, 1601 (1959), also NRL Report 5083, 1958 (unpublished).

⁵ R. O. Bondelid and J. W. Butler, NRL Report 5897, 1963 (unpublished).

⁶ K. L. Dunning, J. W. Butler, and R. O. Bondelid, Phys. Rev. **110**, 1076 (1958).

factors is given elsewhere,⁵ but three of the more important considerations are as follows:

(1) Malfunctions in the analyzer power supply and voltage measuring equipment, such as nonlinearities in the potentiometer and resistor stack, dirty slidewire contacts, temperature changes in the resistor stack and elsewhere, thermoelectric contact potential differences within the measuring circuit, instabilities of the standard cell and working cell, and unbalance between the + and - voltages on the two deflecting plates;

(2) accumulation of an insulating layer on the inner wall of the drift tube between the input slit and the collimating slit of the electrostatic analyzer, and, hence, an accumulation of polarized electric charge on this wall with consequent beam deflection;

(3) accumulation of electric charges (and potential) on the analyzer deflecting plates because of the presence of insulating layers.

The National Bureau of Standards checked the potentiometer and resistor stack for nonlinearity ($<0.01\%$) and checked the standard cell, potentiometer, and resistor stack for absolute calibration (0.01%).

Item (2) was conceived as the possible result of gas molecules being ionized in the drift-tube space between the input slit and collimating slit of the electrostatic analyzer and then depositing onto insulating layers on the drift-tube walls. The earth's magnetic field could serve as a charge polarizer, deflecting positive ions to one side and negative ions to the other. To test this possibility, an external magnetic field was superimposed on this drift-tube space such that the net normal magnetic field was reversed. No effect due to the accumulation of charge on the walls of the drift space was observed on the electrostatic analyzer calibration.

Accumulation of electric charges on insulating layers covering the deflecting plates, item (3), could introduce a nonlinearity as well as an absolute error in the energy calibration of the analyzer. The expected polarity of this charge is such that the energy value observed would be higher than that which would be obtained without the spurious charge. If the spurious charge were a constant, independent of applied voltage, then the energy values obtained would have less percentage error as the applied voltage is increased. Thus, the energy calibration for the H_2^+ beam would give a result which would be too low relative to the H_1^+ beam calibration. Consequently, the possible effects due to the accumulation of electric charges were considered to be very serious both with respect to the absolute calibration of the electrostatic analyzer and with respect to the evaluation of the H_2^+ beam anomalies. In connection with the measurement of absolute bombarding energies of certain reaction thresholds and resonances, we observed that such an accumulation of charges did indeed occur. Therefore, a detailed program was undertaken to study the nature of the effect.

Definitive evidence for the effect of charge accumulation first appeared during preliminary measurements of $T^3(p,n)He^3$ threshold energy.⁷ (The final results reported in Ref. 7 were not influenced by the charge-accumulation effect.)

The manner in which the effect was manifested is as follows. At any time following a period of several hours during which no beam was passed through the electrostatic analyzer a measurement of the $T^3(p,n)He^3$ threshold energy would give a result which we shall call E_{th} . Repeating the measurement continuously would give a series of results each higher than the previous one until, after about 2h, there would be no further increase. The measured threshold energy would return to E_{th} after a waiting period of several hours for the charge to leak off or after the introduction of nitrogen gas at low pressure followed by an ac glow discharge between the deflecting plates. The maximum increase of the measured threshold energy above E_{th} was 0.04% . For the $T^3(p,n)He^3$ threshold energy, this increase requires the equivalent of a uniform charge accumulation on each deflecting plate corresponding to 2V. However, under the assumption of a uniform charge accumulation it is not possible to account for the long time constant of the drift. A simple calculation can be made to determine approximately the time constant from the known pressure in the analyzer (5×10^{-6} torr), the approximate beam current (10^{-7} A), and the following assumptions. (1) All ion pairs created by collisions between the incoming beam and residual gas are collected on the surfaces of the deflecting plates exposed to the beam. (2) No secondary electron emission occurs. (3) Ohm's law is applicable to the insulating layers.

The result is that the time constant should have been about one second. Under the assumption that the principal contribution to the drift came from highly localized insulating areas, it is possible to account for the long time constant provided that the resistivity of the deposited material is about $10^{17} \Omega\text{-cm}$. Some resins have a resistivity of about this amount. When the analyzer was opened and one of the deflecting plates removed, two areas of a few square centimeters each of a dark deposition were observed. One of these spots was near the input at a point where the beam would strike the outer plate if no voltage were applied to the deflecting plate, and the other spot was near the output of the analyzer. A general light-color deposition of material was observed covering the remaining portions of the deflecting plates in the vertical region occupied by the beam during normal operation. A fine abrasive was used to remove the hardened deposit, and the analyzer was reassembled and recalibrated. The result for the threshold energy was now within 0.01% of E_{th} , and there was no observable long-term drift. Furthermore, the ac

⁷ R. O. Bondelid, J. W. Butler, C. A. Kennedy, and A. del Callar, Phys. Rev. **120**, 887 (1960).

gaseous glow discharge would cause no shift in calibration. Possible conclusions are (1) that the light-colored layer caused an error in calibration of as much as 0.01%, and probably this layer had a very short time constant for charge accumulation and (2) that the larger error, 0.04%, and the long time constant were caused by the darker areas on the deflecting plates.

After the conclusion of the above investigation the midpoint of the rise of the H_2^+ beam thick-target (p, γ) yield curve was still observed to be 0.05% lower than that predicted from the H_1^+ beam result.

B. Thin Targets

Even after the aforementioned considerations and checks, it was still not certain that the displacement was not due to some unconsidered aspect of the instrumentation. As a further check the resonance energy was determined with extremely thin targets. It was expected that if we had properly considered all significant aspects of the instrumentation, the peak of the thin-target H_2^+ beam yield curve would occur at the position predicted from the H_1^+ beam result. *Indeed, this check did result in agreement between the H_1^+ and H_2^+ beam observed thin-target peaks within an uncertainty of about 0.01%!* Thus, the linearity of the instrument and technique were established beyond question, and the apparent displacement of the midpoint of the rise of the H_2^+ beam thick-target yield curve from resonance energy has, therefore, been shown to be a real effect in nature.

C. Other Anomalies

The family of curves shown in Fig. 1 was obtained from the E -series family of targets and the H_2^+ beam at the 992-keV resonance in the $Al^{27}(p, \gamma)$ reaction. Inspection of these curves reveals five additional anomalies. (1) The peaks of the moderately thin-target yield curves are not displaced from each other and from resonance energy by an amount as great as was previously expected. (2) Even the "thick" target has a peak, or hump, near resonance energy. (3) The asymmetries of the moderately thin-target yield curves are very pronounced, greater than expected on the basis of target nonuniformities and ordinary fluctuations in energy losses determined from the H_1^+ beam yield curves with the same targets; and the full widths at half-height of these moderately thin-target yield curves are greater than predicted from the full width at half-height of an extremely thin-target H_2^+ beam yield curve and the target thicknesses and energy-loss fluctuations obtained with the H_1^+ beam on the same targets. (4) The "step" in the thick-target yield curve shows a definite asymmetry about its midpoint. (5) The "thick-target plateau" for target $E-1$ is not really a plateau but a secondary slow rise.

During the course of the experiments, a number of models were invented in attempts to explain the anom-

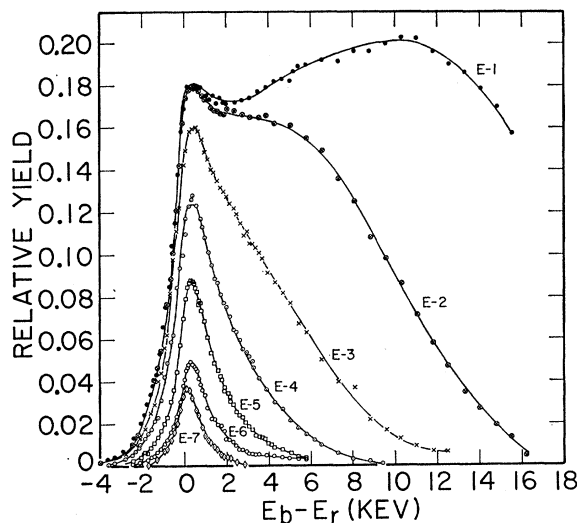


FIG. 1. The experimental H_2^+ beam yield curves of the E -series aluminum targets near the resonance energy of 992 keV. The targets vary in thickness from 17.8 keV for $E-1$ to 0.31 keV for $E-7$, each different from the adjacent member by about a factor of 2. Note the failure of the peaks to shift as much as half the target thickness, the thin-target asymmetry which becomes more pronounced as a function of target thickness, the thick-target leading-edge asymmetry, the dip just above resonance energy for the thick-target curve, and the slow rise following the dip. The abscissa energies have been converted to the H_1^+ energy scale.

alies of Fig. 1. For each model further experiments were devised specifically to test the validity of a crucial feature of that particular model. In most cases, the model failed to pass the test, but these further experiments led to additional information concerning the behavior of H_2^+ beams.

D. Inert Coatings

One series of tests involved the coating of the targets by thin layers of inert material, chosen to be copper. These tests with the coated targets indicated new discrepancies which contributed to an understanding of the behavior of the H_2^+ beam in targets.

In one set of experiments one particular thick target was first used to obtain the usual H_1^+ and H_2^+ beam excitation curves over the region of the 992-keV resonance. Then a thin layer of copper was evaporated over the layer of aluminum, and another pair of H_1^+ and H_2^+ beam yield curves was obtained. Then, another thin layer of copper was evaporated onto the same target and another pair of yield curves was obtained. The H_2^+ beam yield-curve displacement (determined for the midpoint of the rise) for the first layer was measured to be 900 eV, an amount which is about the same as that obtained for the H_1^+ beam yield-curve displacement, 870 eV. However, for the combined copper layers, the apparent energy loss suffered by the H_2^+ beam in traversing the layers was significantly greater than for the H_1^+ beam, 2020 and 1710 eV, respectively.

It is also interesting to compare the experimental

resonance widths for the several different cases. Here the term "width" for the thick targets is used to represent the interquartile interval. The H_1^+ beam yield curves for all three target situations and the H_2^+ beam yield curve for the uncoated target can be used to "predict" the width of the H_2^+ beam coated-target yield curves. For the H_1^+ beam, the observed widths are 270, 700, and 1160 eV, respectively. For the H_2^+ beam the observed widths are 1200, 1950, and 2780 eV, respectively. The "predicted" widths for the last two cases are 1360 and 1650 eV, respectively. Thus, it appears that the fluctuations in energy losses suffered by the H_2^+ beam in traversing the copper coatings are relatively much greater than for the H_1^+ beam.

Two different thin targets of equal thickness were used for a somewhat similar set of experiments except that a layer of copper was evaporated onto only one target. The coated-target energy shift (determined for the peak) was 290 eV for the H_1^+ beam and 320 eV (referred to the H_1^+ scale) for the H_2^+ beam. As with the first coating over the thick target, the displacements for the two different beams are about the same within experimental uncertainties. However, the width (here the term "width" refers to the full width of the thin-target resonance peak at half-height) of the H_2^+ beam yield curve for the coated target is significantly greater than "predicted" from the width measurements with the H_1^+ beam, 1650 eV compared with 1310 eV for the "predicted" width.

In another pair of thin-target measurements, a thicker layer of copper was evaporated. The energy displacement of the H_2^+ beam yield-curve peak was 2620 eV, an amount which is considerably greater than that for the H_1^+ beam, 2160 eV. And again, as in every previous case, the increased width of the resonance peak is much greater for the H_2^+ beam, 3180 eV compared with the "predicted" width of 1860 eV.

The results of the copper coating experiments may be summarized as follows. (1) The coatings cause a shift in energy of the resonance peaks or midpoints. (2) For the thinner coatings, the H_1^+ and H_2^+ beam yield curves are shifted in energy about equal amounts (both beams referred to the H_1^+ energy scale). (3) For the thicker coatings, the H_2^+ beam yield curves are shifted in energy relatively more than the H_1^+ beam yield curves. (4) The apparent fluctuations in energy losses of the H_2^+ beam in penetrating the inert coating are relatively much greater than those for the H_1^+ beam. This effect applies to both thin and "thick" coatings, but is more pronounced for thicker coatings (greater than about 1 keV).

E. H_1^+ and H_1^0 Beams from the H_2^+ Beam

Further efforts to gain an understanding of the behavior of H_2^+ beams led to the use of a gas cell for stripping the H_2^+ beam into a neutral H_1^0 component and an H_1^+ component, referred to hereinafter by the

symbol $H_1^+)_s$. Both He and N_2 were used (at different times) as the stripping gas. The cell, 10 cm long, had diaphragms at each end for beam passage. The entrance aperture was 5 mm long with a diameter of 1 mm; the exit aperture was 20 mm long with a diameter of 2 mm. The system was differentially pumped. A typical cell pressure was about 10^{-2} Torr. A magnetron magnet was used to separate the various components of the beam: H_1^0 , $H_1^+)_s$, and residual H_2^+ .

The H_1^0 and $H_1^+)_s$ beam intensities were more limited than those of the unmodified hydrogen molecular-ion beam, and factors such as counting rates and "signal-to-noise" ratios were consequently reduced for the H_1^0 and $H_1^+)_s$ beams. Nevertheless, yield curves (not illustrated) were obtained with the use of the electrostatic analyzer. Because of the lack of statistical accuracy for the points on these curves and because extreme linearity, beam-energy precision, and resolution were not required for the measurements with the gas cell, additional yield curves, shown in Fig. 2 were obtained with the use of the magnetic beam-energy analyzer alone. In addition to the stripped-beam thick-target yield curves, Fig. 2 also shows the H_2^+ beam thin- and thick-target yield curves for comparison and calibration purposes.

There are several features of these curves worth particular note. (1) The midpoints of the rise for the thick-target $H_1^+)_s$ and H_1^0 yield curves are *not displaced* from the true resonance energy (more than 0.01%). (2) The stripped-beam yield curves are *symmetric* about the resonance energy. (3) The stripped-

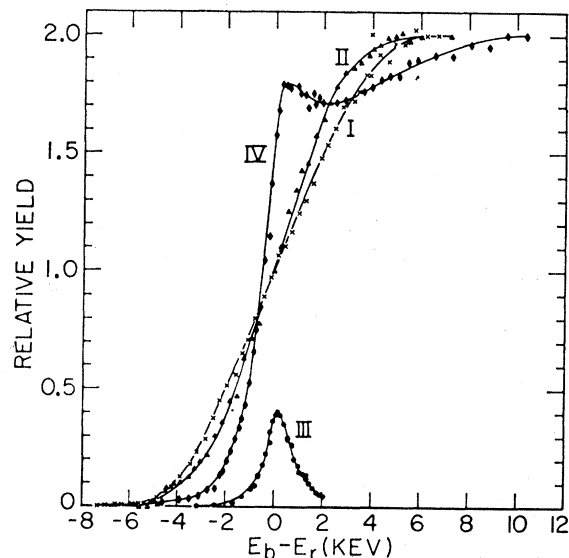


FIG. 2. Experimental yield curves for thick aluminum targets, 992-keV resonance, gas-stripped beams. Curve I, $H_1^+)_s$ beam. Curve II, H_1^0 beam. Curve III, H_2^+ beam, thin target. Curve IV, H_2^+ beam, thick target. Curves III and IV are for comparison purposes. Note the symmetry of the stripped-beam curves and the lack of a displacement of the midpoint of the rise. Also note the fact that curve I is broader than curve II.

beam yield curves *have much larger widths* than those for the direct H_2^+ beam. (4) The H_1^+ beam gives a somewhat wider resonance yield curve than the H_1^0 beam.

Thus, we have apparently eliminated two discrepancies, the midpoint energy displacement and the asymmetry, but we have introduced another discrepancy! The average energy loss of the beam in penetrating the gas cell was only about 17 eV; thus, this loss could not (according to previous concepts) possibly have introduced a distribution in energy loss with a full width at half maximum of 4 keV!

IV. QUALITATIVE EXPLANATION OF THE ANOMALIES OBSERVED WITH THE H_2^+ BEAM

There were no displacement or asymmetry discrepancies when either very thin targets or stripped beams were used. Thus, these discrepancies are associated with the combination of the H_2^+ beam and thick targets.

The energy displacements for thin coatings were about the same for H_2^+ and H_1^+ beams while for thick coatings the energy displacement for the thick coating was significantly greater for the H_2^+ than for the H_1^+ beam. Also, apparent fluctuations in energy losses for the H_2^+ beam were considerably greater than for the H_1^+ beam when either an inert coating or the gas cell was placed in front of the target. An important clue to the nature of the discrepancy was thus the time factor. When the H_2^+ beam was stripped by the gas, the hydrogen molecular ion had approximately 10^{-7} sec to dissociate before the dissociation particles struck the target. However, inside the target, the H_2^+ molecule had only about 10^{-14} sec before it (or the dissociation components) had lost enough energy to be of no interest in the yield at bombarding energies near the resonance energy. (A 1-MeV proton in aluminum loses energy at the rate of about $600 \text{ eV}/10^{-15} \text{ sec}$.) Therefore, a basic re-examination of the fundamental processes involved in the breakup of the H_2^+ molecule was undertaken and led to a satisfactory explanation.

The H_2^+ molecule is the simplest of the molecular structures and, therefore, has received intensive theoretical study. Figure 3 shows potential energy curves^{8,9} for a few of the electronic configurations of the H_2^+ molecule, and also shows some of the vibrational eigenvalues¹⁰ for the $J=0$ (parahydrogen) state.

Now let us consider the mechanism of dissociation of the hydrogen molecular ion. Salpeter¹¹ has made approximate calculations for the dissociation of H_2^+ molecules of a few MeV in collision with gas molecules. These estimates by Salpeter show that only about 1% of the dissociations of these H_2^+ molecules in collision with hydrogen gas occur by excitation of the inter-

nuclear vibrations. (Dissociation by excitation of nuclear vibrations requires an energy transfer of about 2.8 eV.) The mechanism for dissociation of the other 99% of the H_2^+ molecules is by excitation from the ground electronic state to the higher electronic-state configurations of H_2^+ . If we assume that the H_2^+ molecule is in the lowest vibrational level of the ground electronic state, and if we also assume that in a collision the Franck-Condon principle will apply (i.e., the internuclear separation distance does not change during the collision and concomitant excitation to one of the higher electronic states), it can be seen from the potential-energy diagram that excitation to the lowest repulsive state ($2p\sigma_u$ state) requires an energy transfer of about 11.8 eV. The H_2^+ molecule thus excited will then dissociate into a free proton and a neutral hydrogen atom, following the potential "hill," with a total final separation kinetic energy of about 9.0 eV in the c.m. system. The next lowest state is the $2p\pi_u$ state, and about 18.2 eV are required for excitation to this state. (This state is weakly bound if excitation occurs at certain large internuclear distances, but for present purposes it may be regarded as a repulsive state.) For excitation to this state and all higher electronic states, Salpeter points out that dissociation results in a free proton, a neutral hydrogen atom in an excited state, and some kinetic

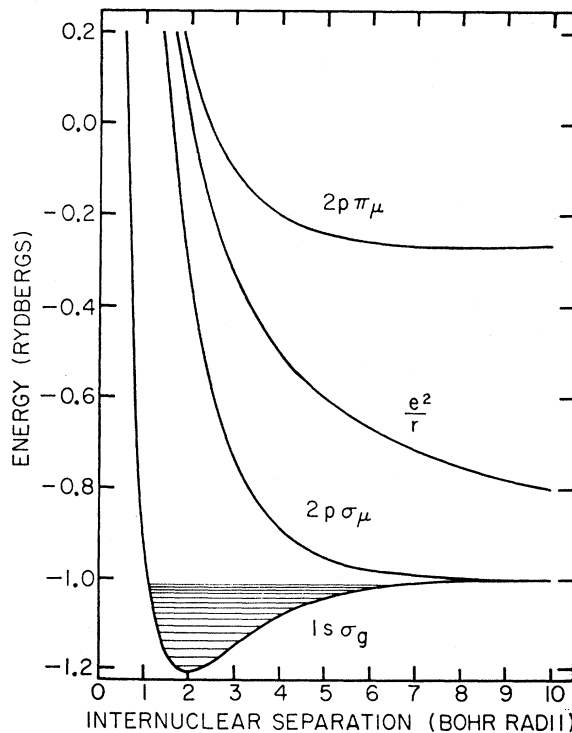


Fig. 3. Potential-energy curves for various electronic state configurations of the H_2^+ molecule. The e^2/r curve has been drawn one Ry below its proper position to conserve space and to make comparisons easier. Vibrational levels are illustrated for a parahydrogen molecule ion in the ground electronic-state configuration.

⁸ E. Teller, Z. Physik **61**, 458 (1930).

⁹ D. R. Bates, K. Ledsham, and A. L. Stewart, Phil. Trans. Roy. Soc. London **246**, 215 (1953).

¹⁰ S. Cohen, J. R. Hiskes, and R. J. Riddell, Jr., Phys. Rev. **119**, 1025 (1960).

¹¹ E. E. Salpeter, Proc. Phys. Soc. (London) **63A**, 1295 (1950).

energy. An energy transfer of 30 eV (or more) is required for excitation to continuum states, which then result in two free protons and a free electron.

Calculations of the cross sections for the dissociation of H_2^+ and D_2^+ by a vacuum carbon arc have been made by Alsmiller,¹² who shows that the principal modes of dissociation in the arc are by excitation from the ground state to the $2p\sigma_u$ and the $2p\pi_u$ states. Excitation to other states is essentially negligible. Other authors have investigated some aspects of the dissociation cross sections and angular distributions for the dissociation process.

The above discussion indicates the principal modes of dissociation of H_2^+ molecules under circumstances different from those prevailing in the present experiments. Thus, it is not known precisely what happens when the H_2^+ molecules enter the target lattice; i.e., it is unknown what fraction of the H_2^+ molecules are excited to each state or to the continuum. It is of interest to estimate the time required for dissociation. For excitation to the $2p\sigma_u$ state, a semiclassical calculation shows that for 90% of the potential energy to be converted to kinetic energy (protons assumed to be initially stationary) a time of 3.7×10^{-15} sec is required. If it is assumed that dissociation takes place by prompt removal of the electron so that the potential-energy function becomes $E = e^2/r$ (see Fig. 3), then the time required for 90% of the potential energy to be converted to kinetic energy is 17×10^{-15} sec.

Since the time required for 90% energy conversion of the proton and neutral hydrogen atom following excitation of the H_2^+ molecule to the $2p\sigma_u$ state is about the same as the time required for a proton to lose about 2.5 keV in the aluminum target, the time-factor clue mentioned above acquires added significance.

In the case of the gas-cell experiments, enough time was available to the dissociating molecules so that all of the potential energy available to the dissociation process was transformed into kinetic energy before the particles reached the target. For each proton which received an increase in energy, there was a corresponding proton which received an equal decrease in energy; and, thus, the resulting distribution of energies in the bombarding beam was symmetric about E_b . Because the energy spread which results from the dissociation process is due to the addition of velocity vectors, the amount of the extra energy spread is the order of several keV even though there is available only a few eV to the dissociation process. This relatively large energy spread is sufficient to mask the effects due to fluctuations in energy loss,² and the yield curves obtained with the H_1^0 and H_1^+ beams are reasonably symmetric about resonance energy, and the midpoint of the rise in the thick-target yield curve is located very near resonance energy.

However, when a solid target is bombarded by the H_2^+ beam, the resulting dissociation takes place inside the target, thus leading to an energy distribution whose width increases as a function of depth of penetration of the beam into the target. The result is an overall asymmetric yield curve for thick targets.

In the front layers of the target, a significant portion of the beam is gaining energy from the dissociation process faster than it is losing energy through ordinary energy-loss interactions. This effect is especially important when $E_b \leq E_r$, for it causes some protons to remain near resonance energy for abnormally long times and some to pass through resonance energy twice. Furthermore, even for values of E_b sufficiently below E_r , that essentially none of the protons in the incident beam have energies great enough to contribute significant gamma-ray yield, some protons will gain enough net energy inside the target to reach resonance energy and thus contribute significant gamma-ray yield. It is this latter result that gives the long slow rise beginning more than 5 keV below resonance energy (Curve IV, Fig. 2).

A similar line of reasoning explains the observed result that the position of the midpoint of the rise is significantly below resonance energy.

At values of E_b about 2000 eV above E_r , the yield is less, even for a thick target, than for E_b values only a few hundred eV above E_r for the following reasons. (For simplicity, we shall consider only those molecules whose internuclear axes are aligned with the direction of motion.)

In the latter case ($E_r \leq E_b \leq E_r + 500$ eV), there is extra yield from the "leading" protons as discussed above, but this extra yield is approximately compensated by the yield loss from the "trailing" protons. This yield loss results from the fact that the "trailing" proton passes through the resonance energy zone more quickly (if it initially is at or above resonance) than it normally would from the usual energy-loss process alone. So it makes fewer nuclear passes while it is in the resonance energy zone.

In the former case ($E_b \approx E_r + 2000$ eV), there is no extra yield from the leading protons because they start above resonance energy and gain net energy for some time. Their contribution to the yield comes after dissociation is essentially complete, and they pass through the resonance energy zone at the normal rate of energy loss. But the yield loss from the trailing protons still exists because the trailing protons, losing energy from the usual process plus the dissociation process, very quickly pass through it.

The above processes explain both (1) the failure of the peaks of moderately thin targets to shift and (2) the presence of the hump on thick targets.

As the bombarding energy is increased still further, more and more of the trailing protons still have energies above resonance even after the dissociation process is essentially complete. Therefore, they pass through the resonance energy zone at the normal rate of energy loss,

¹² R. G. Alsmiller, Jr., Oak Ridge National Laboratory Document 2766, 1959 (unpublished).

thus making a relatively greater contribution to the yield. The result is a slowly rising yield, as a function of bombarding energy, until all of the trailing protons pass through the resonance energy zone at the normal rate. This second rise in yield is shown clearly in Figs. 1 and 2. For a sufficiently thick target, a plateau would eventually be reached, but none of the E series targets is thick enough to exhibit one. The yield curve for target $E-1$ essentially reaches the "thick-target plateau" level, but its plateau is very short.

The results with the copper-coated targets can be visualized qualitatively with the dissociation mechanism. The enhanced broadening effect of the copper coating on the H_2^+ beam thin- and thick-target yield curves as compared with the H_1^+ beam yield curves is due to the fact that part of the dissociation of the H_2^+ molecules occurs in the inert copper coatings thus eliminating the yield which would otherwise have been obtained from the front of the target where the beam-energy spread is the smallest.

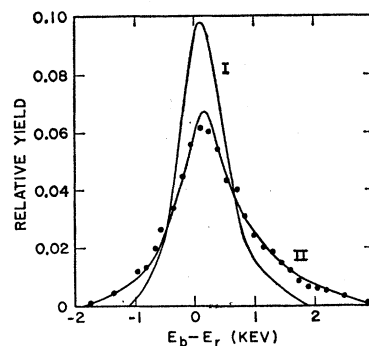
For thick targets of aluminum with the thicker copper coating, it was observed that the shift of the H_2^+ beam yield curve midpoint due to the coating was also greater than for the H_1^+ beam. As shown in the preceding discussion, the anomaly of the low midpoint for thick targets and the H_2^+ beam depends upon the dissociation acceleration occurring in the aluminum target. If the dissociation acceleration occurs before the protons reach the aluminum target, there is no anomalously low midpoint, as seen from the gas-cell results. If a copper layer is sufficiently thick, the dissociation acceleration will be complete before the protons reach the aluminum. Thus, the shift of the midpoint of the H_2^+ beam yield curve for a copper-coated target includes two factors, the normal shift due to fluctuations in energy loss plus the shift due to the obviation of the anomalously low midpoint related to the dissociation process.

V. CALCULATED YIELD CURVES

It is possible for one to calculate the H_2^+ beam yield-curve shapes for all target thicknesses by beginning with a beam of H_2^+ molecules and considering in microscopic detail the physical processes occurring as the beam penetrates the target. Such calculations have been performed for the E -series targets, and two examples are shown in Figs. 4 and 5 for targets $E-7$ and $E-1$, respectively.

The mechanism of dissociation of the H_2^+ molecules was assumed to be as follows. The H_2^+ molecules enter the target lattice in various vibrational states and are excited to various electronic repulsive states by interactions with the lattice electrons. The internuclear separation distance does not change during the excitation process in accordance with the Franck-Condon principle. The probability for such excitation is represented by the term $1 - e^{-\alpha x}$, where α is the product of the interaction cross section and the number of atoms per

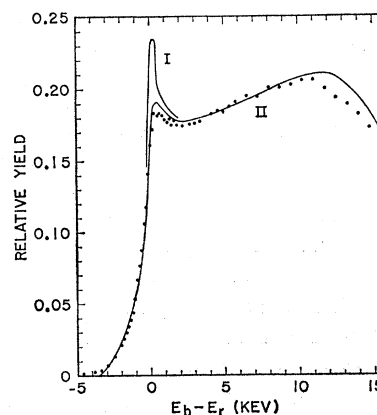
FIG. 4. Calculated yield curves and datum points for target $E-7$, H_2^+ beam. The abscissa values have been converted to the H_1^+ energy scale. Curve I was calculated for a pure aluminum target; curve II, a completely oxidized target.



cm^2 , and x is the penetration distance into the target. The two dissociation components gain energy in the c.m. system according to the repulsive-state potential curve. Further interactions with the lattice electrons result in eventual excitation of the H_2^+ molecule to the e^2/r "state" or stripped condition. The dissociation continues until it is complete. Since at small values of r , the various electronic repulsive curves are essentially parallel to the e^2/r curve, the dissociation as described gives a similar overall result as if the original excitation had been to the e^2/r curve. And since the e^2/r curve is mathematically much simpler to handle than the excited electronic-state curves, the calculations were made under the assumption of a one-step process to the e^2/r curve.

The initial distribution of proton energies in the bombarding beam is a function of effective beam analyzer resolution, internal kinetic energy of the protons in the H_2^+ molecules, and the distribution of internuclear axis orientations. After the H_2^+ molecules have penetrated far enough into the target to lose an energy of about 200 eV, the width of the initial distribution is small compared with the broadening introduced by dissociation of the molecules. Therefore, the effect of the initial proton energy distribution was taken into account as follows. The effective energy width of the beam due to dissociation alone was computed. If this width was less than 500 eV, it was assumed that the effect of the initial energy distribution would cause the

FIG. 5. Calculated yield curves and datum points for target $E-1$, H_2^+ beam. The abscissa values have been converted to the H_1^+ energy scale. Curve I was calculated for a pure aluminum target; curve II, a pure target except for a 150-eV layer of 67% aluminum oxide on the surface beneath which is a 150-eV layer of 33% aluminum oxide.



over-all energy distribution to be 500-eV wide. Thus, the width of the undisturbed component $e^{-\alpha x}$ of the initial beam remained constant at 500 eV, while the width of the disturbed component $1-e^{-\alpha x}$ changed continually through the target as the internal kinetic energy of the disturbed H_2^+ molecules increased according to the e^2/r potential curve.

The yield curves were computed under the following particular assumptions and procedures. The average population of vibrational levels of the H_2^+ molecules corresponds to the $v=3$ level. Effectively, the probability distribution of initial r_0 values (internuclear separation distances) is flat, and the overall yield curve may be obtained by combining with equal weight the yield curves resulting from r_0 values of 1.4, 2.0, and 3.0 Bohr radii. The internuclear axis has an isotropic orientation probability, and the cross section for excitation is independent of this orientation. The H_2^+ ion loses energy in the target at the same rate as two independent protons. The densities of target materials are the handbook values of 2.7 g/cm³ for pure aluminum and 3.7 g/cm³ for aluminum oxide. Possibly some assumptions compensate for others; e.g., the average vibrational level might be under $v=3$, but the $v=3$ assumption might compensate for the independence of excitation cross section on internuclear axis orientation.

The following effects were neglected: The effect of target electrons on the dissociation process, fluctuations in energy losses of the H_2^+ molecules and the dissociation components, molecular rotational energy, and intrinsic resonance width.

Curve I of Fig. 4 shows the calculated yield for target *E-7*, assumed to be pure aluminum. The experimental data obtained with the H_1^+ beam on target *E-7* agreed with the H_1^+ beam yield curve calculated under the assumption of complete oxidation of the target.² Therefore, curve II was computed for a completely oxidized target. The effect of the oxidation of the target on the calculated curve is to broaden it because the oxidized target is thicker in terms of both energy loss and penetration time. Since more time is required for the H_2^+ molecules to penetrate target *E-7* if it is oxidized than if it is pure, more internal kinetic energy is realized before the molecules leave the other side of the target. Even though the oxidized target *E-7* is about 600-eV thick, the peak of the yield curve is displaced only about 160 eV from resonance energy. Whereas with thin targets bombarded by the H_1^+ beam, the asymmetry of the yield curves was due to fluctuations in energy losses of the protons in the target, the asymmetry of the yield curves of thin targets bombarded by the H_2^+ beam is due primarily to the changing internal energy of the H_2^+ molecules in repulsive electronic states.

Yield curves computed for thin targets *E-3* through *E-6* (not illustrated) similarly agreed with the experimental data, showing only very small displacements of their peaks from resonance energy and similar asym-

metries, thus, explaining the anomalies observed with the H_2^+ beam on thin and moderately thin targets.

For target *E-1*, several yield curves were computed for several assumed surface conditions. Most of these curves were quite similar except in the immediate vicinity of resonance energy. So only the curve having best agreement with the data in the vicinity of resonance energy is shown in full in Fig. 5.

Curve I was calculated for a pure target. Apparently, if the target surface had been pure, a very pronounced overshoot would have resulted in the experimental data. But the weak overshoot implies that the yield from the front layers of the target, when the incoming beam is sharpest, is attenuated. An oxide layer on the surface does have this effect because it dilutes that part of the target by about a factor of two. A calculated curve for a 150-eV layer of 100% aluminum oxide on the surface still showed somewhat too much overshoot. But the curve for a 300-eV layer of 100% aluminum oxide showed too little overshoot, essentially none at all.

Curve II was calculated for a 150-eV layer of 66% aluminum oxide on the surface beneath which is a 150-eV layer of 33% aluminum oxide. The agreement is excellent for all energies except very near resonance and on the decreasing-yield slope. The agreement at resonance would be improved if slightly more than 67% oxidation were assumed in the first 150-eV layer or if this layer were assumed slightly thicker; and the lack of complete agreement at the high-energy side may be attributed, at least partly, to the effect of fluctuations in energy losses in the target (these fluctuations were ignored in the calculations).

Although target *E-1* is not actually a thick target, it is at the threshold of being thick because its yield curve reaches the final thick-target plateau level, even though the plateau is very short.

Curve II predicts all of the anomalies observed with the H_2^+ beam on a thick target: the asymmetry of the leading edge, the displacement of the midpoint of the rise, the overshoot, the slow rise following the overshoot, and the less steepness associated with the trailing edge than with the leading edge.

VI. APPLICATION TO RESONANCE-ENERGY DETERMINATION

The H_2^+ beam can be used for accurate calibration of bombarding-beam energy analyzers provided that either extremely thin targets are used (thinner than about 500 eV) or the effects of dissociation are taken into account with intermediate or thick targets.

A. Thin Targets

If extremely thin targets are used and if the H_1^+ and H_2^+ beam yield-curve peaks are compared on the same energy scale, the positions of the peaks will agree within 0.01%. From the experimental data for target *E-7* and from the absolute calibration parameters of

the electrostatic analyzer, the positions of the peaks for the H_1^+ and H_2^+ beams occur at 992.10 and 992.17 keV, respectively, thus differing by only 0.007%. These values include no correction, theoretical or otherwise, for any shift of the peak from true resonance energy.

B. Thick Targets

If thick targets are used, there are two methods which will give the position of resonance within an uncertainty of about 0.01%. The first is empirical, and therefore much simpler, although slightly less reliable. The procedure is to extrapolate the slow rise of the experimental yield curve after the dip to intersect with the steep rise; this point of intersection is within 0.01% of resonance energy.

The second procedure is to calculate a yield curve as done herein and thus determine the position of the midpoint of the rise with respect to resonance energy. Reasonable assumptions may be made about target surface conditions, and the energy of the midpoint is not nearly so sensitive to surface conditions as the overshoot. Such a computation can be performed by hand in a period of a few hours.

VII. DISCUSSION

A preliminary account of part of the present paper (the energy displacement of the H_2^+ beam thick-target yield curve and the asymmetry of the same curve) has been published in abstract form.¹ In the intervening period, work closely related to the present series of experiments has been performed at two other laboratories. The University of Oslo group has observed some of the anomalous features of the H_2^+ beam thick-target excitation curves and published their results.¹³ The

¹³ S. L. Andersen, K. Gjötterud, T. Holtebekk, and O. Lönsjö, *Nucl. Phys.* **7**, 384 (1958).

University of Wisconsin group has also observed some of the anomalous features with H_2^+ beams, and they have published their results.¹⁴⁻¹⁶

Of the anomalies observed, the most important was the "energy shift" of the midpoint of the rise in the thick-target yield curve. In order to confirm the "shift" as a real effect in nature, we undertook a detailed program of examining all the parameters of the electrostatic analyzer for linearity and compensating effects as a function of voltage applied to the deflecting plates (and, thus, particle energy). These checks and procedures, as described in Sec. II, are a necessary and primary means of proving an analyzer sufficiently linear to establish the observed "energy shift" with H_2^+ beams as a real effect. The internal and external magnetic field corrections in Eq. (1), for example, are about the same magnitude as the apparent midpoint displacement.

After the primary checks mentioned above, the secondary check is to measure the resonance energy with the H_2^+ beam on an extremely thin target and to compare the resonance energy thus obtained with that predicted from the measurement with the H_1^+ beam and the absolute calibration parameters. As described herein, we made this check and obtained agreement within 0.01% between the two measurements.

ACKNOWLEDGMENTS

For their valuable contributions, we are grateful to the following persons: C. A. Kennedy and A. del Callar for help during the experimental phase of the problem; K. L. Dunning and R. G. Glasser for many valuable suggestions and discussions.

¹⁴ P. F. Dahl, D. G. Costello, and W. L. Walters, *Bull. Am. Phys. Soc.* **5**, 406 (1960).

¹⁵ P. F. Dahl, D. G. Costello, and W. L. Walters, *Nucl. Phys.* **21**, 106 (1960).

¹⁶ W. L. Walters, D. G. Costello, J. G. Skofronick, D. W. Palmer, W. E. Kane, and R. G. Herb, *Phys. Rev.* **125**, 2012 (1962).